Three-Dimensional Tumor Dosimetry for Hepatic Yttrium-90-Microsphere Therapy

P.L. Roberson, R.K. Ten Haken, D.L. McShan, P.E. McKeever, and W.D. Ensminger

Departments of Radiation Oncology, Pathology and Internal Medicine, University of Michigan Medical Center, Ann Arbor, Michigan

The nonuniformity of dose deposition for hepatic ^{90}Y-microsphere therapy is believed to play an important role in the relative sparing of normal liver tissues. To help study this issue, three-dimensional dose calculations have been performed for the VX2 tumor model in the rabbit treated with hepatic arterial administration of ^{90}Y-glass microspheres (^{90}Y-MS). Colored, nonactivated spheres of similar size to ^{90}Y-MS were injected into the hepatic artery to mimic the treatment deposition of ^{90}Y-MS. Sample blocks of treated liver were serially sectioned (200 μm thickness), fixed and photographed showing the position of the colored microspheres. The microsphere positions were digitized into a three-dimensional treatment planning system, and three-dimensional dose calculations were performed. A 2-mm diameter liver tumor nodule receiving 15 times more microspheres than nearby normal liver resulted in tumor-to-normal-tissue (TNT) calculated dose ratios of 2.6 (average dose) and 1.9 (minimum dose). The nonuniform microsphere distribution resulted in a dose gradient over the nodule with a minimum value which was less than one half the average dose. The relative dose deposition in the vicinity of the tumor nodule does not fully reconcile the known liver tolerance dose derived from uniform irradiation with the large calculated average doses tolerated with this type of therapy.

J Nucl Med 1992; 33:735–738

Liver involvement by cancer occurs frequently, causing considerable morbidity and mortality. External radiation treatment is of palliative benefit for large symptomatic liver tumors. However, local control of intrahepatic metastases is limited by the low radiation tolerance of normal hepatic parenchyma, reported to have a threshold of 30 Gy of external radiation to avoid a significant occurrence of radiation-induced hepatitis (*1*). The use of hepatic arterial administration of ^{90}Y-glass microspheres to selectively irradiate hypervascular regions of tumor tissue can improve the tumor/normal tissue (TNT) therapeutic ratio. Studies in dogs (*2*) and humans (*3,4*) have found minimal dose-related toxicity at relatively high average liver doses (up to 150 Gy in dogs and 100 Gy in humans).

The nonuniformity of dose deposition is believed to play an important role in the relative sparing of normal liver tissues (*5,6*). To permit an investigation of the distribution of dose deposition, the distribution of microspheres was studied using hepatic arterial infusion for the VX2 tumor model (*7*) in New Zealand white rabbits.

METHODS

The locations of the glass microspheres cannot be precisely determined because they are transparent. Estimates of their spatial distribution were determined by injection of nonactivated, colored microspheres, which were visualized on magnified photographic projections of tissue sections. The positions of the microspheres were individually digitized, and the resulting three-dimensional microsphere distribution was used to calculate dose distributions employing a ^{90}Y dose point kernel.

Tissue Sample Preparation

A detailed description of the tumor development, microsphere injection and sample preparation has been published elsewhere (*8*). The tumor model employed was the VX2 tumor cell line grown in the liver of New Zealand white rabbits. A 0.2-ml tumor suspension (1×10^6 cells) was injected into the right and left lobes of the liver. Isolated VX2 tumor nodules developed 2 wk postinjection.

Blue-dyed, 27-μm diameter polystyrene microspheres (Polybead Polystyrene Microspheres; Polysciences, Inc., Warrington, PA) were used to mimic their radioactivated analogs, glass (or plastic) microspheres of similar size (22-μm diameter for the glass microsphere Therashere, Theragenics Corp., Atlanta, GA). The commercially produced polystyrene microsphere solution consisted of a 2.5% sphere concentration (approximately 2.3×10^6 microspheres per ml). The liver samples analyzed were taken from a rabbit which received a 0.5 ml microsphere solution through hepatic arterial injection.

The liver tissue samples were cut serially in 200-μm thick sections using a vibrating microtome. The sections were mounted on a glass slide, coverslipped and photographed. The photography resulted in a series of 35-mm slide photographs of liver sections of approximately 3 mm by 4 mm. The distance scale was determined by photographing a hemacytometer grid pattern.

Dosimetry

The colored photographic slides of tissue sections were projected onto a wall-mounted digitizer pad, resulting in a total magnification factor of 150. The microspheres were identified

Received Aug. 9, 1991; revision accepted Dec. 19, 1991.

For reprints contact: Peter L. Roberson, PhD, Department of Radiation Oncology, University of Michigan Medical School, UH-B2C490, Box 0010, 1500 E. Medical Center Dr., Ann Arbor, MI 48109.

and their positions digitized. The third microsphere coordinate was entered as the center of each 200-μm sample slice. The microsphere position data were entered into the VAX 8800 computer using a brachytherapy treatment planning program (*9*). For convenience, the calculation scale was adjusted to millimeter rather than the typical centimeter scale by appropriate modification of the distance scale of the radial dependence and the normalization constant of the ^{90}Y dose point kernel (*10*).

Three-dimensional source distributions were determined for two samples, one with a tumor nodule and another of adjacent normal tissue. The slides were serially aligned to define a block of tissue with dimensions of approximately 3 × 4 × 2 mm^3. A contour around the tumor nodule was entered for each slide. The contours were connected to form a three-dimensional tumor volume. The nodule was assumed to extend only through the slides composing the sample. The surrounding tissue not included in the original samples was assumed to be normal liver.

The range of the most energetic ^{90}Y beta particles is larger than the sample dimensions. Therefore, a representative calculation of dose required an estimation of the dose due to beta particles emitted from microspheres outside of the tissue sample. The distribution of microspheres in the surrounding tissue was estimated using the density and frequency of microsphere clusters in the normal liver sample. A cluster was defined as all microspheres within a 0.5-mm cube. The normal liver cluster sizes ranged from 0 to 8 microspheres with 92% of the cubes containing zero microspheres. The coordinates and number of spheres in each cluster in the surrounding tissue were chosen at random, weighted by the probability of the occurrence of each cluster size, while keeping the mean sphere density approximately constant. Four independent random samplings were analyzed to estimate the range of nodule dose contribution from the microspheres in the surrounding tissue.

Dose calculations were performed using a dose point kernel for ^{90}Y (*10*), assuming that the dose distribution for each microsphere was well represented by a point source dose distribution. A nominal activity per microsphere of 10 nCi was chosen. Dose attributed to each source with full decay was calculated for three-dimensional grid points within the tissue volume. Dose values at each grid point were summed for all sources (inside and outside of the volume) to yield the full three-dimensional dose distribution. Isodose curves were drawn by computer interpolation of grid point values.

The heterogeneity of the dose distribution is represented by differential dose-volume histograms. The differential dose-volume histogram is a plot of the fractional volume (dV/V) assigned doses within an incremental dose interval (dD). The area under the histogram curve is unity, representing the full volume of the tissue sample.

RESULTS

The average microsphere densities in the normal liver and tumor nodule samples were 1.5 and 22 microspheres per mm^3, respectively. However, the maximum number of microspheres per cluster in the 3 × 4 × 2 mm^3 sample tissue volumes were 8 spheres for the normal liver sample and 13 spheres for the tumor nodule sample. The microsphere distribution for the normal liver was relatively more nonuniform than that for the tumor nodule. Isodose curves superimposed on photographs of representative normal liver and tumor sections (Fig. 1) show higher values in the vicinity of microspheres. The calculated dose is higher in the tumor nodule (light-colored region in right panel of Fig. 1) compared to the normal tissue.

The average calculated doses to normal liver and to the 2-mm diameter tumor nodule assuming local deposition of emitted energy were 27 Gy and 410 Gy, respectively. The average doses correspond to those calculated using the MIRD schema (*11*) if the (inappropriate) assumptions of uniform source distribution and local dose deposition were used. However, a significant portion (80%) of the energy from the microspheres in the tumor nodule contributed to the dose in the surrounding tissue, resulting in an average nodule dose of 71 Gy and a higher dose in the normal liver near the tumor nodule compared to more distant normal liver tissue. The nonuniformity of the dose inside of the tumor is illustrated by a dose profile taken through the center of the tumor nodule (Fig. 2). The dose outside of the tumor gradually declines over a 2–3-mm interval to dose levels characteristic of the surrounding liver. The width of the region with higher dose is a function of the penetrating power of the beta particles.

The contribution to the average tumor dose from the surrounding tissue not included in the samples (assumed to be normal liver tissue) was estimated to range between 17 and 24 Gy using random selection of source clusters. This represents 80% of the average dose to normal liver and 30% of the average dose to the tumor nodule. The random cluster sampling generated dose nonuniformities on the same scale observed for the normal tissue sample. Barring an unexpected macroscopic variation of microsphere density in nearby tissue, the uncertainty in the calculated doses due to the missing normal tissue is relatively small (approximately 12% of the average normal tissue dose and 5% of the average tumor dose).

The differential dose-volume histograms for the three-dimensional dose distribution calculations (Fig. 3) showed relatively broad ranges of doses for the normal tissue and more so for the tumor nodule. The average doses differ by a factor of two to three (27 versus 71 Gy) and the minimum dose by a factor of two (16 versus 31 Gy). This contrasts with the relative magnitudes of microspheres (1.5 versus 22 mm^{-3}). The discrepancy is due to the beta energy escaping the nodule. The minimum doses are smaller than the average doses by a factor of two for both samples. The presence of a relatively sharp minimum dose is due to the greater range of the beta particles (3.5 mm average) compared to the characteristic scale of the microsphere nonuniformity.

DISCUSSION

The deposition of glass microspheres may be affected by the greater density of glass (~2.5 g/cm^3) compared to blood. If present, this effect would be expected to make the distribution of spheres less uniform due to the in-

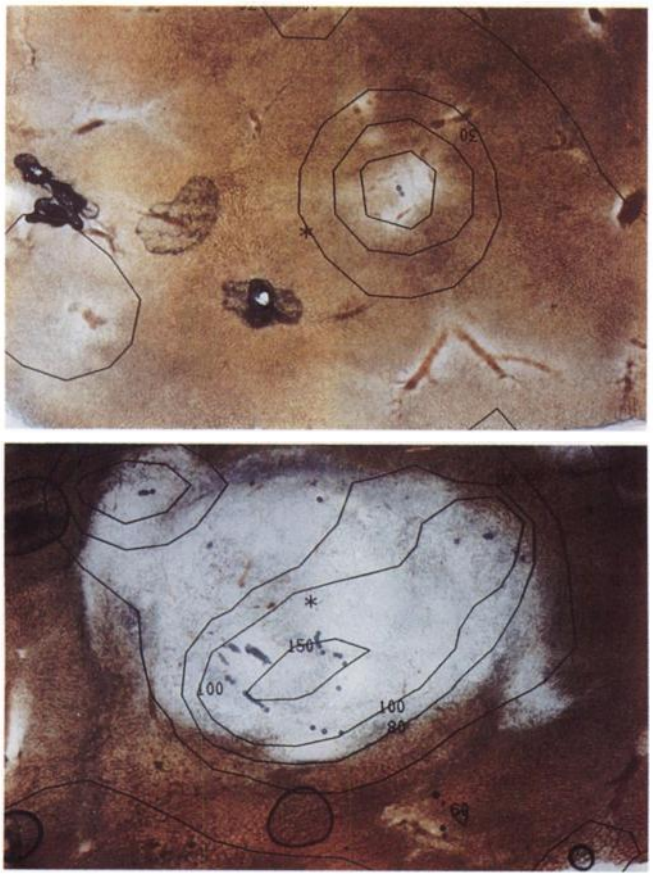

FIGURE 1. Isodose curves superimposed on tissue section photographs. (Left) Normal tissue (20, 30, 40, 60 Gy). (Right) Tissue with tumor nodule (20, 40, 60, 80, 100, 150 Gy). The higher dose regions are in the vicinity of microspheres in the illustrated or adjacent sections.

creased difficulty of achieving a uniform mix with the blood. The use of plastic, activated microspheres may be advantageous because the physical density is approximately isodense with blood, although previous use of

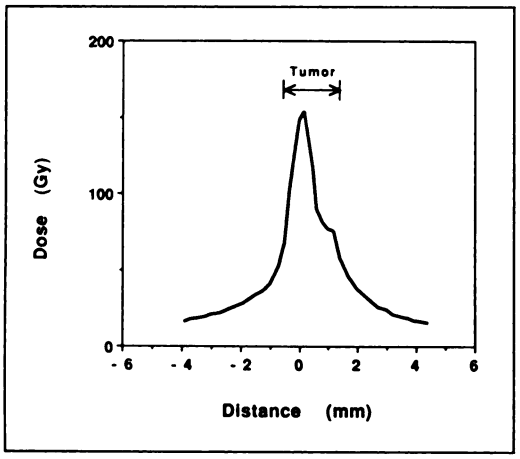

FIGURE 2. Dose profile through center of tumor nodule. The extent of the tumor is indicated by the bar. The origin was defined near the center of the tissue sample.

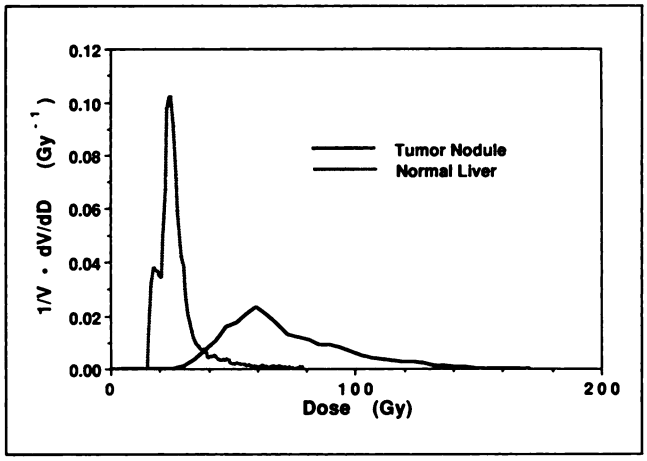

FIGURE 3. Differential dose-volume histograms for normal liver and tumor nodule. The ordinate values are the differential fractional volumes (dV/V) containing the differential dose increment (dD). The curves are normalized so that their integral areas are unity representing the full volume.

ceramic or resin microspheres have resulted in excessive uptake of yttrium by the bone marrow due to leaching of free yttrium (*2*). The average microsphere ratio between tumor and normal liver would imply a favorable dose ratio if the assumptions of uniform activity distribution and local dose deposition were valid. However, the microspheres are not deposited uniformly and the maximum range of the ^{90}Y beta particles exceeds the dimensions of the tumor nodule. This results in a dose nonuniformity in normal tissue and tumor (Fig. 3) and a relatively low average TNT dose ratio.

The penetrating power of the ^{90}Y beta particles does have some mitigating effect on the nonuniformity. A nonuniform activity distribution can be converted into a relatively uniform dose distribution, if the scale of the nonuniformity is less than 2–3 mm. The intercluster distances previously reported (*8*) for a tumor nodule extends up to 2 mm, while for normal liver tissue, there is a significant portion above 3 mm. This distribution scale of microspheres favors the beta particle penetration depth obtained from ^{90}Y. The dose to tumor is made more homogeneous without requiring the surrounding tissue to be similarly concentrated with activity. Also, the dose deposited in normal tissue adjacent to the tumor nodule due to the range of the beta particles may provide the beneficial effect of increasing the margin of elevated dose in the vicinity of tumor.

A tumor nodule with a diameter of 2 mm is about as small as would benefit from the range of the ^{90}Y beta particles. Smaller diameter nodules would experience a greater portion of the beta energy being deposited in the surrounding tissue. Also, there is the possibility for the nodule to be too small to experience a significant increase in blood flow to trap larger portions of the microspheres than are deposited in nearby normal liver tissue.

The nonuniformity of the microsphere deposition re-

sulted in a dose gradient in the nodule extending down to 30 Gy, or less than half of the average dose and one-tenth of the dose calculated according to the MIRD schema assuming only nonpenetrating radiations. Even though the minimum tumor dose was relatively low, the TNT dose ratio (therapeutic ratio) between the minimum tumor and normal liver doses was significant (a factor of two). The therapeutic ratio can be described as a comparison of dose ranges (Fig. 3). The minimum dose to tumor may be predictive of final therapy outcome (i.e., cure), but may not be the best predictor of tumor response. Likewise, the minimum dose to normal liver may be related to its capacity for recovery, but the average dose may also have some validity. For these reasons, we quote ratios of the average doses (2.6) and the minimum doses (1.9).

The basic functional unit of the liver is the lobule, having a diameter of approximately 2 mm (*5*). Measured lobule diameters ranged from 0.5 mm to 2.5 mm for rabbit liver and from 0.5 mm to 3 mm for human liver. While the measurements may be influenced by some sections taken obliquely to the lobule axis, lobule sizes for rabbit and human livers are similar. The microspheres deposited in normal liver tissue tend to locate at the periphery of the lobules, resulting in microsphere cluster separations at least on the order of 2 mm and frequently larger. The penetration depth of the ^{90}Y beta particles produces a minimum dose level that is a function of the average microsphere density as long as the scale of nonuniformity is not more than 2 to 3 mm. The minimum dose regions are farthest from the microsphere clusters and are therefore likely to be in the vicinity of the lobule centers. The minimum dose to normal liver may be most significant because the lobule centers are generally credited as the main site of hepatic damage during external radiation exposure (*1,5*).

The large average doses estimated to be tolerable with this type of therapy (*2,3,4,6*) are not fully explained by the minimum normal tissue dose being half of the average normal tissue dose. It is possible that for treatments performed on patients with significant tumor burden, the average dose to normal liver was substantially below the average liver dose due to the hypervascularity in tumor tissue. When the normal liver dose was estimated separately, the maximum average dose was 75 Gy with up to 147 Gy delivered to the tumor (*6*). This average normal liver dose is not substantially larger than twice the external beam tolerance dose.

From their study of a dog model, Wollner et al. (*2*) estimated that the human liver can easily tolerate 100 Gy. Although factors other than dose distribution may be significant, this apparent discrepancy could be reconciled if the distribution of microspheres was more macroscopically nonuniform (*6*). That is, a more significant nonuniformity may be present due to the vasculature of the major vessels creating a nonuniform deposition on a larger scale. The minimum dose to normal liver tissue could be substantially smaller than indicated by the normal liver sample studied here. Normal liver samplings at many locations are being performed to investigate this possibility.

The uncertainty in the three-dimensional dose calculation for the normal liver can be reduced by using larger sample sizes. Analyses of tissue sections on the order of 1 cm^3 are planned.

ACKNOWLEDGMENT

Supported in part by NIH grant CA-33825.

REFERENCES

1. Ingold JA, Reed GB, Kaplan HS, Bagshaw, MA. Radiation hepatitis. *Am J Roentgenol Radium Ther Nucl Med* 1965;93:200–208.
2. Wollner I, Knutsen C, Smith P, et al. Effects of hepatic arterial yttrium-90 glass microspheres in dogs. *Cancer* 1988;61:1336–1344.
3. Herba MJ, Illescas FF, Thirlwell MP, et al. Hepatic malignancies: improved treatment with intraarterial Y-90. *Radiology* 1988;169:311–314.
4. Houle S, Yip TK, Shepherd FA, et al. Hepatocellular carcinoma: pilot trial of treatment with Y-90 microspheres. *Radiology* 1989;172:857–860.
5. Russell JL, Carden JL, Herron HL. Dosimetry calculations for radioactive yttrium-90 used for treatment of liver cancer. *Endocurietherapy/Hyperthermia Oncology* 1988;4:171–186.
6. Burton MA, Gray BN, Klemp PF, Kelleher DK, Hardy N. Selective internal radiation therapy: distribution of radiation in the liver. *Eur J Cancer Clin Oncol* 1989;25:1487–1491.
7. Kidd JG, Rouse PA. A transplantable rabbit carcinoma originating in a virus-induced papilloma and containing the virus in masked or altered form. *J Exp Med* 1940;71:813–838.
8. Pillai KM, McKeever PE, Knutsen CA, Terrio PA, Prieskorn DM, Ensminger WD. Microscopic analysis of arterial microsphere distribution in rabbit liver and hepatic VX2 tumor. *Selective Cancer Therapeutics* 1991;7:39–48.
9. Fraass BA, McShan DL. 3-D treatment planning. I. Overview of a clinical planning system. In: Bruinvis IAD, ed. *The use of computers in radiation therapy.* (North-Holland), Amsterdam: Elsevier Science Publishers B.V.; 1987:273–276.
10. Prestwich WW, Nunes J, Kwok CS. Beta dose point kernels for radionuclides of potential use in immunoradiotherapy. *J Nucl Med* 1989;30:1036–1046 and 30:1739–1740.
11. Loevinger R, Berman M. A revised schema for calculating the absorbed dose from biologically distributed radionuclides. In: *MIRD Pamphlet No. 1, revised.* New York: Society of Nuclear Medicine; 1976.